Experimental Charge Density Study of Estrogens: 17β-Estradiol·Urea

Damon Parrish,† Elizabeth A. Zhurova, Kristin Kirschbaum, and A. Alan Pinkerton*

Department of Chemistry, University of Toledo, 2801 West Bancroft Street, Toledo, Ohio 43606

Received: August 30, 2006; In Final Form: October 13, 2006

To relate the molecular electrostatic potential to the biological activities of estrogens, a comparative charge density study of different derivatives has been initiated. The second completed charge density analysis of this series for 17β-estradiol·urea is presented here. This is a large organic system with 52 atoms in a noncentrosymmetric space group, therefore special tools such as an optimal coordinate system and slow, initially constrained refinement have been used to accomplish this study. Our results for the urea molecule reasonably agree with previous experimental and theoretical results. In the 17β-estradiol molecule, the oxygen atoms appear to be close to sp^3 in shape, exhibiting two consistent, distinct lone pairs despite different chemical environments. No significant interaction of the hydroxyl group oxygen with the π orbitals of the aromatic ring is observed. Analysis of the electrostatic potential revealed that the negative potential in the lone pair region of the two oxygen atoms is quite different. The topological analysis of the electron density has been performed, and the atomic charges have been estimated.

Introduction

Estrogens are known to be responsible for the development of secondary sexual characteristics, as well as effecting growth, differentiation, and function of a wide range of tissues.[1] It has also been shown[2] that some estrogens are responsible for the initiation and progression of certain types of breast cancer. These molecules have the ability to bind as ligands to the estrogen receptor in the first of many steps which may result in the activation (agonistic effect) or repression (antagonistic effect) of genes critical to the mechanism of tumor growth. While the mechanism by which estrogens influence cancer is currently unknown, subtle changes in the chemical structure of estradiol and the other estrogens are known to elicit different biological responses in the development of cancer. It has been suggested[3] that the agonistic/antagonistic responses of the different estrogens can be related to such physical properties as their electrostatic potential.

A comparative charge density study of a series of estrogen derivatives has thus been initiated in our group, with the primary goal of relating the electronic and physical structure of the molecules to their biological action. In addition to molecular properties, charge density studies provide significant fundamental information about the functional groups and their constituent atoms, helping to investigate basic chemical principles of small organic molecules in general. The first study of this series on the estrone crystal has been recently reported.[4] The current paper will pay particular attention to the hydroxyl groups of the estrogen molecule. The hydroxyl groups are the most chemically interesting portion of the estrogen molecule, and their interaction with the receptor is thought to be critical for biological activity.

Described here is the charge density study of 17β-estradiol·urea. This particular crystal was chosen for two reasons. First, 17β-estradiol (E_2) is the most common naturally occurring estrogen and is typically the standard to which all other estrogenic activities are related. E_2 demonstrates an agonistic response in *in vitro* tests, which typically utilize the estrogen receptor in either competitive yeast or human cell assays.[5,6] Second, the system contains a urea molecule that has been extensively studied, both theoretical and experimental charge density studies having been performed on this molecule.[7−14] This provides a direct means of validating our methodology and the results obtained for E_2. A deformation electron density map for E_2 has been previously reported,[15] but no detailed analysis has been published.

Experimental Section

Data Collection and Reduction. Crystals were grown by slow evaporation as described by Duax in the original publication of the crystal structure.[16] A clear, colorless crystal of approximate dimensions $0.35 \times 0.37 \times 0.40$ mm^3 was attached to a 30 μm carbon fiber. X-ray diffraction data were collected at 100.0(1) K on a Bruker Platform Diffractometer equipped with a SMART 6000 CCD area detector located 7.12 cm from the goniometer center. An Oxford Cryostream system was used to cool the crystal. The crystal was irradiated with graphite monochromated Mo Kα radiation ($\lambda = 0.71073$ Å). Omega (0.3°) scans were carried out at four phi settings and three detector positions, resulting in more than 7400 frames. A frame time of 60 s was used for the low-angle setting, and 180 s for the medium- and high-angle settings. The complete experimental protocol has been deposited. The intensities were integrated with the program SAINT.[17] The program SORTAV[18] was used for outlier determination and averaging the data. Other experimental details are listed in Table 1.

Least-Squares Refinements. The crystal structure was resolved, and the spherical atom model was refined by using the program SHELXTL.[19] The 17β-estradiol and urea molecules are shown in Figure 1. All hydrogen atoms were located from the difference Fourier maps and their positions have been refined. The results of this refinement served as the starting point

* Address correspondence to this author, E-mail: apinker@uoft02.utoledo.edu.
† Current address: Laboratory for the Structure of Matter, Naval Research Laboratory, Washington, DC 2037.

10.1021/jp065638x CCC: $33.50
Published on Web 11/29/2006

TABLE 1: Crystal Information and Experimental Details.

formula	$C_{18}H_{24}O_2 \cdot CH_4N_2O$
formula weight	332.43
crystal system	orthorhombic
space group	$P2_12_12_1$
a	7.9022(9) Å
b	9.2228(10) Å
c	24.589(3) Å
volume	1792.06 Å^3
μ	0.08 mm^{-1}
Z	4
T	100.0(1) K
λ	0.71073 Å
$(\sin\theta/\lambda)_{max}$	1.165 Å^{-1}
no. of reflecns	
collected	92584
rejected outliers	2986
unique	19258
included in the refinement[a]	9884
data completeness	89.4%
av redundancy	4.5
R_{int}	0.0295
spherical refinement	
R_1	0.0395
wR_2	0.1007
multipole refinement	
$R(F)$	0.0168
$R(F^2)$	0.0260
S	1.0994
residual electron density	−0.08/0.10 e Å^{-3}

[a] $I > 4\sigma(I)$, measured more than twice.

for the aspherical atom refinements that were performed with the XD software package.[20]

The aspherical atom model[21] used in further refinements is based on atom-centered multipoles, hence a local coordinate system is required for each atom in the system. For the core structure of the estrogen molecule, this was set up by using a standard estrogen coordinate system, which takes advantage of the shape of certain multipoles to increase the stability of the initial multipole refinements.[22] The defining vectors for the oxygen atoms of the estrogen molecule were directed to bound atoms. The coordinate system setup for the urea molecule has been deposited.

Before the aspherical refinements were begun, the hydrogen atom positions were corrected by extending the X−H distances to their neutron bond lengths[23] ($C_{sp^2}H = 1.08$ Å, $C_{sp^3}H = 1.10$ Å, $C_{sp^3}H_2 = 1.09$ Å, $C_{sp^3}H_3 = 1.06$ Å, OH = 0.97 Å, $N_{sp^2}H_2 = 1.01$ Å), and these distances were fixed in subsequent refinements. To stabilize the initial stages of the multipole refinement and provide an additional reference point for the topological analysis, a solid state theoretical calculation (DFT/B3LYP/6-31G(d,p)) using the Crystal98 program[24] has been performed at the experimental geometry obtained after preliminary multipole refinements. Theoretical X-ray structure factors were generated, and the multipole model was again refined. The results have been deposited. The κ' values thus obtained for the C(19), O(3), and all H atoms were then used for the refinements over the experimental data, which provided a more stable refinement process.

A well-known correlation exists between the displacement parameters and the κ parameters of hydrogen atoms, only allowing the κ parameters to be refined when the thermal parameters of the hydrogen atoms are known.[25] To avoid this problem, fixed κ values ($\kappa_H = 1.20$) were used, while the thermal parameters were allowed to refine.[26,27] Optimum positional and atomic displacement parameters for the non-hydrogen atoms were obtained from a high-angle refinement ($\sin\theta/\lambda > 0.7$ Å^{-1}), and those for hydrogens from a low-angle refinement ($\sin\theta/\lambda < 0.7$ Å^{-1}). The multipole model parameters were refined against data with $\sin\theta/\lambda < 1.0$ Å^{-1}, while the scale factor was refined over all data.

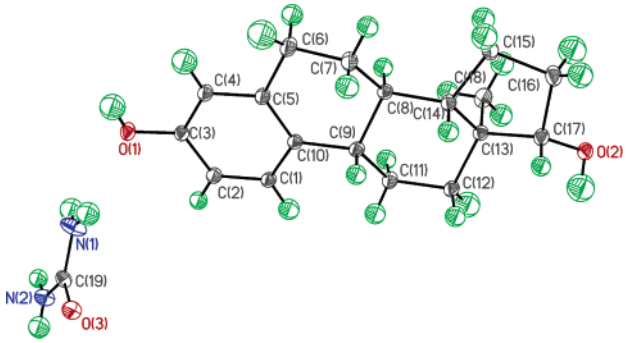

Figure 1. 17β-Estradiol and urea molecules showing 50% probability thermal ellipsoids at 100 K.

Initially, chemical constraints were applied and only the most significant multipoles were considered.[22] By the end of the refinement, all non-hydrogen atoms were treated up to the octupole level with no chemical constraints. To account for the hydrogen bonding in the crystal, all dipole and quadrupole parameters were refined for the H(1O), H(2O), and the H atoms of the urea molecule, while only the dipoles and one P_{20} quadrupole parameter were refined for all other hydrogens. The H(1, 2, 4), H(8, 9, 14), all H(A, B), and H(18(A, B, C)) were constrained to group values. The electroneutrality constraint was independently imposed on both of the molecules. Final structural information, such as atomic coordinates, thermal parameters, bond lengths, angles, and multipole parameters, has been deposited.

Topological Analysis, Atomic Charges, and Electrostatic Potential. A topological analysis of the electron density was performed based on the Quantum Theory of Atoms in Molecules (QTAIM)[28] with the program WinXPRO.[29,30] Quantitative critical point[31] analysis on all covalent and hydrogen bonding interactions, as well as oxygen lone pair densities, has been performed. The atomic zero-flux surfaces[28] have been localized and atomic charges were integrated within the basins. This method allows an unambiguous partitioning of the molecules into the respective atoms, leading to the additivity and transferability of its properties.[32] The integrated atomic charge $q(\Omega)$ over the atomic basin Ω can be defined as a difference between nuclear Z_Ω and electronic $N(\Omega)$ charges:

$$q(\Omega) = Z_\Omega - N(\Omega), \qquad N(\Omega) = \int_\Omega \rho(\mathbf{r})\, d\tau$$

The calculation of the electrostatic potential (ESP) was also performed with the program WinXPRO. The ESP can be calculated as

$$V(\mathbf{r}) = \sum_A \frac{Z_A}{|\mathbf{R}_A - \mathbf{r}|} - \int \frac{\rho(\mathbf{r}')\, d\mathbf{r}'}{|\mathbf{r}' - \mathbf{r}|}$$

where Z_A is the charge on nucleus A located at $\mathbf{R}_A$. The construction assembles positive charges at the nuclei and a continuous distribution of electrons. The calculations were performed based on a single β-estradiol molecule isolated from the crystal.

Results and Discussion

Packing. The molecular structure and hydrogen-bonding pattern were found to be the same as described by Duax.[16] The

TABLE 2: Geometrical Information for the Hydrogen Bonds[35]

A···H−D	*d*(A···D), Å	∠AHD, deg
O(1)···H(1NB)−N(1)	2.9772(4)	137.9(4)
O(1)···H(2NB)−N(2)	3.0083(4)	167.1(4)
O(2)···H(1O)−O(1)	2.6706(3)	171.1(4)
O(2)···H(2NA)−N(2)	3.1011(4)	167.2(4)
O(3)···H(2O)−O(2)	2.6400(3)	164.9(4)
O(3)···H(1NA)−N(1)	2.8219(4)	168.9(4)

TABLE 3: Expansion/Contraction (κ and κ') Parameters for the 17β-Estradiol·Urea Crystal

atoms	κ	κ'
O(1), O(2)	0.971(2)	0.78(3)
C(3)	1.017(6)	0.98(3)
C(17)	1.028(5)	0.87(2)
C(1), C(2), C(4)	1.002(3)	0.83(1)
C(5), C(10)	1.014(3)	0.86(2)
C(6)−C(9), C(11)−C(18)	1.003(2)	0.80(4)
H atoms (C−H and O−H)	1.2	1.34[a]
C(19)	1.026(6), 0.97(1)[b]	0.89[a]
O(3)	0.981(2), 0.98(1)[b]	1.28[a]
N(1), N(2)	0.988(4), 0.98(1)[b]	0.95(3)
H atoms (N−H)	1.2, 1.02(2)[b]	1.23[a]

[a] Fixed to the value refined over the theoretical data. [b] Reported by Zavodnik et al.[7]

packing of this structure results in a formation of six hydrogen bonds ranging in donor−acceptor length from 2.64 to 3.10 Å; these are listed in Table 2. The O(1) atom acts as an acceptor in two hydrogen bonds with hydrogens of two independent urea molecules (H(1NB) and H(2NB)). The H···O vectors of these hydrogen bonds are pointed almost directly at the positions of the lone pairs of O(1) (see the Supporting Information). The O(2) atom has a very similar hydrogen-bonding structure to O(1) in which it acts as an acceptor in two hydrogen bonds and a donor in one. The hydrogen atoms from the O(1) atom of another independent E_2 molecule and H(2NB) of a urea molecule line up almost directly with the lone pair positions of O(2). Topological analysis yielded a (3,−1) critical point and a bond path[33] for each hydrogen−acceptor interaction, verifying the true bonding interaction in these hydrogen bonds.[34] The complete table of results from hydrogen bond topology has been deposited.

κ Parameters. The coefficients of expansion/contraction of the spherical valence and deformation densities, κ and κ' parameters respectively are shown in Table 3. The grouping of individual atoms was based on the atom type, hybridization, and chemical environment. A total of 11 κ sets were utilized to allow the necessary flexibility while attempting to maintain a minimum number of parameters. As mentioned earlier, the hydrogen atoms' κ values were fixed at 1.20, and the κ' values for the C(19), O(3), and all H atoms were fixed to the values refined over the theoretical structure factors. All other κ values were allowed to refine during the least-squares minimization. For the urea molecule, our κ parameters perfectly match those reported by Zavodnik et al.[7] for the O(3) and N atoms, whereas there is a significant difference for the C(19) atom.

Atomic Charges. The net atomic charges were derived directly from the monopole populations of the multipole model, as well as from the integration of the electron density within the atomic basins as described by the QTAIM theory. As mentioned earlier, the urea molecule gives us the opportunity to compare our data with previous theoretical and experimental results.[7−14] Among the list of references, only refs 7 and 8 provide direct information for comparison. The atomic charges in this work are in a fair qualitative agreement with the values

TABLE 4: Net Atomic Charges for the Atoms of 17β-Estradiol·Urea[a]

atom	$q(P_v)$	$q(\Omega)$	atom	$q(P_v)$	$q(\Omega)$
		17β-estradiol			
O(1)	−0.63(4)	−1.41	H(1)	0.17(2)	0.08
O(2)	−0.51(4)	−1.18	H(2)	0.17(2)	0.10
C(1)	−0.17(4)	−0.02	H(4)	0.17(2)	0.14
C(2)	−0.23(5)	−0.05	H(6A)	0.02(3)	−0.02
C(3)	0.06(8)	0.24	H(6B)	0.02(3)	0.07
C(4)	−0.28(5)	−0.06	H(7A)	0.05(3)	−0.06
C(5)	0.10(4)	0.03	H(7B)	0.05(3)	−0.01
C(6)	−0.09(4)	−0.02	H(8)	0.10(2)	0.02
C(7)	−0.08(4)	0.05	H(9)	0.10(2)	0.00
C(8)	−0.08(3)	0.03	H(11A)	0.09(2)	0.01
C(9)	−0.10(3)	−0.03	H(11B)	0.09(2)	−0.01
C(10)	0.09(4)	0.08	H(12A)	0.07(3)	0.01
C(11)	−0.08(4)	0.10	H(12B)	0.07(3)	0.00
C(12)	−0.01(4)	0.14	H(14)	0.10(2)	−0.01
C(13)	0.07(3)	0.11	H(15A)	0.05(3)	−0.01
C(14)	0.00(3)	0.06	H(15B)	0.05(3)	0.04
C(15)	−0.08(4)	0.00	H(16A)	0.07(3)	0.01
C(16)	−0.15(4)	0.01	H(16B)	0.07(3)	0.05
C(17)	0.35(5)	0.51	H(17)	0.02(3)	−0.04
C(18)	−0.13(6)	0.11	H(18A)	0.02(3)	−0.07
H(1O)	0. 20(4)	0.62	H(18B)	0.02(3)	−0.07
H(2O)	0.13(4)	0.60	H(18C)	0.02(3)	−0.04
		urea[b]			
O(3)	−0.48(3)	−1.25	H(1NA)	0.15(4)	0.50
	−0.23(7)	−1.48		0.21(4)	0.55
N(1)	−0.17(8)	−1.29	H(1NB)	0.15(4)	0.49
	−0.30(9)	−1.57		0.21(4)	0.53
N(2)	−0.13(8)	−1.22	H(2NA)	0.15(4)	0.50
	−0.30(9)	−1.57		0.21(4)	0.55
C(19)	0.19(7)	1.70	H(2NB)	0.15(4)	0.51
	−0.03(13)	2.46		0.21(4)	0.53
		molecule			
E_2	0.00	0.07	urea	0.00	−0.07

[a] $q(P_v)$: net atomic charges derived directly from the monopole populations of the multipole model. $q(\Omega)$: charges integrated over the atomic basins. [b] Second line for the urea molecule: $q(P_v)$ reported by Zavodnik et al.,[7] $q(\Omega)$ reported by Gatti et al.[8] $L_{err} = (\sum L_\Omega^2/N_{atoms})^{1/2} = 0.00054$ au, $L_\Omega = -1/4(\nabla^2\rho)_\Omega$.[37]

reported by Zavodnik et al.[7] and Gatti et al.[8] (Table 4). The difference (including the difference in the κ (C19) value) can be attributed to the different hydrogen-bonding scheme in the E_2·urea crystal compared with that in crystalline urea, as well as to correlations between the multipole parameters during the least-squares refinement.

Generally, Bader's charges are significantly higher than the charges derived from the monopole populations; this is not surprising due to the different method of calculation. Upon first inspection, a charge of +1.7 e^- for the central carbon of urea seems excessively high. At the same time, there is evidence in the literature, from both theoretical and experimental data, that this is not unreasonable for a carbon surrounded by electronegative oxygen and nitrogen atoms.[8,36]

The net atomic charges for the atoms of the estrogen molecule are as expected for the given atom types and their chemical neighbors. High charges have been obtained for the hydroxyl group O and H atoms, and the carbons next to them, the rest of the molecule being practically neutral. The $q(P_v)$ charges are somewhat higher for the aromatic ring C and H atoms compared with the rest of the molecule. No such tendency is observed for the integrated charges, which include the contributions of all multipoles of the electron density expansion. The $q(\Omega)$ values obtained from the theoretical calculation agree well with the experimental charges and have been deposited.

Topological Analysis. (*a*) *Urea Molecule.* Overall, values of the electron density at the bond critical points, both

TABLE 5: Topological Analysis of the Urea Molecule[a]

	this work				Zavodnik et al.[7]				Gatti et al.[8]	
	experiment		theory		experiment		theory		theory	
bond	$\rho(\mathbf{r})$	$\nabla^2\rho(\mathbf{r})$	$\rho(\mathbf{r})$	$\nabla^2\rho(\mathbf{r})$	$\rho(\mathbf{r})$	$\nabla^2\rho(\mathbf{r})$	$\rho(\mathbf{r})$	$\nabla^2\rho(\mathbf{r})$	$\rho(\mathbf{r})$	$\nabla^2\rho(\mathbf{r})$
C−O	2.79(2)	−32.6(1)	2.65(1)	−29.83(7)	2.54	−18.86	2.57	−7.92	2.57	−7.95
$(C-N)_{average}$	2.43(2)	−25.78(8)	2.28(1)	−23.65(4)	2.54	−37.66	2.35	−27.61	2.36	−27.71
$(N-H)_{average}$	2.49(9)	−40.3(5)	2.33(1)	−36.88(1)	1.82	−31.91	2.34	−47.06	2.34	−47.23

[a] The units for the electron density, $\rho(r)$, are e Å^{-3}, and for the Laplacian, $\nabla^2\rho(r)$, e Å^{-5}.

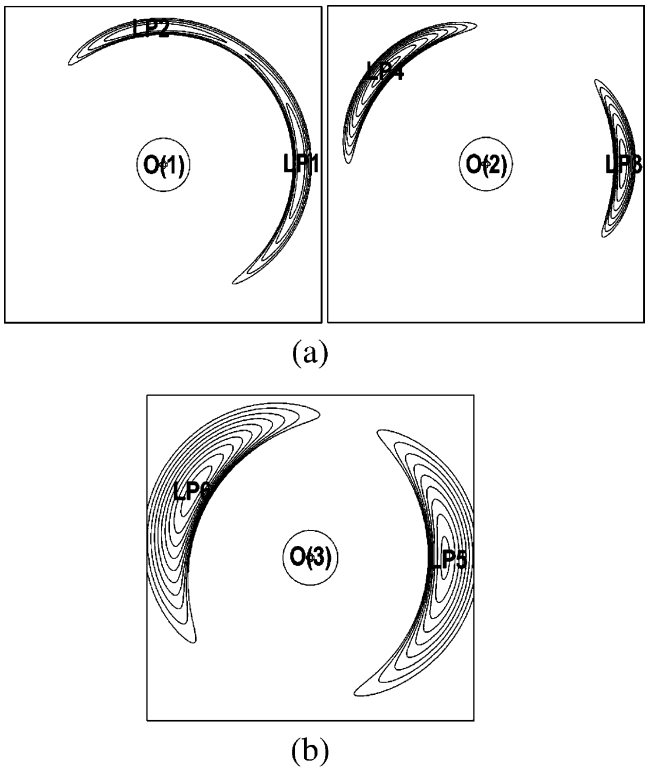

Figure 2. Negative part of the Laplacian in the plane of the lone pairs for the O(1) and O(2) atoms (a) and for the O(3) atom (b). Contour intervals are −2 e Å^{-5} starting at −100 e Å^{-5} for O(1) and O(2), and −10 e Å^{-5} starting at −80 e Å^{-5} for O(3).

experimental and theoretical, are in fair agreement with those reported by Zavodnik et al.[7] and Gatti et al.[8] (Table 5). Zavodnik et al.[7] showed significant differences (∼0.5 e Å^{-3}) between the theoretical and experimental electron densities at the (3,−1) critical point for the N−H bond of the urea molecule. The $\rho(\mathbf{r})$ values in this study are closer to the theoretical values. The difference in the Laplacian values at (3,−1) critical points between experimental and theoretical values is much bigger, showing the sensitivity of the electron density curvature to the different approaches to its estimation, including the deficiency of the multipole model.[38,39]

A critical point search was also performed in the Laplacian, $\nabla^2\rho(\mathbf{r})$, to find the charge density concentrations associated with the lone pairs on the urea oxygen. These critical points are (3,+3) in type, indicating that $\nabla^2\rho(\mathbf{r})$ is a local minimum at $\mathbf{r}_c$. The Laplacian plot in the plane of the lone pairs of the O(3) atom can be seen in Figure 2. The angle between the lone pairs, being greater than 140° (Table 6), is much larger than the ideal trigonal planar geometry in agreement with VESPR theory. The inconsistency between the angles in the experimental and theoretical cases is most likely due to the shallow curved shape of the Laplacian in the lone pair region. An extremely small change in $\nabla^2\rho(\mathbf{r})$ could easily move the critical point by 5−10°. The difference in the Laplacian values between the experimental and theoretical results can also occur due to correlations between the electronic and displacement parameters, not completely avoided in the least-squares refinement. Gatti et al.[8] also found two (symmetry related) (3,+3) critical points in the Laplacian, corresponding to the urea oxygen lone pairs with the $\nabla^2\rho(\mathbf{r}_c) \approx 146$ e Å^{-5} at 0.337 Å from the O(3) nucleus. Our data (Table 6) closely agree with this result, especially our theoretical data, although the urea molecule in the present case does not lie on a special position as it does in the urea crystal, therefore there is no symmetry restriction on any properties, including the electron lone pair concentrations.

(*b*) *E_2 Molecule.* Topological analysis of the covalent bonds of the estrogen molecule demonstrated the characteristic (3,−1) critical points, with expected $\rho(\mathbf{r}_c)$, $\nabla^2\rho(\mathbf{r}_c)$, and ellipticity values given the hybridization and connectivity. The complete list of all bond critical point properties has been deposited. The average $\rho(\mathbf{r}_c)$ values are 1.86 e Å^{-3} for the C−O bonds, 2.15 e Å^{-3} for $C_{ar}-C_{ar}$, 1.62 e Å^{-3} for C−C, 1.84 e Å^{-3} for C−H, and 2.70 e Å^{-3} for O−H. The critical points are well centered for most of the homonuclear C−C bonds, and proportionally displaced away from the more electronegative atom in the heteronuclear bonds. All these values are in the expected range found in the literature.[4,36,40−45] As in estrone, an intramolecular H(1)···H(11A) bonding interaction has been found in the E_2 molecule; its features are discussed elsewhere.[4]

Critical points in the Laplacian corresponding to the lone pairs of both hydroxyl oxygen atoms are of special interest. The $\nabla^2\rho(\mathbf{r})$ maps for the lone pair regions for the O(1) and O(2) atoms are shown in Figure 2, and the deformation electron density maps have been deposited. As in the urea molecule, for the O(2) atom, the angles between the lone pairs agree with VESPR theory in that they are larger than the ideal tetrahedral value. They are found a little smaller for the O(1) atom in the experimental case. As was mentioned before, the differences between the experiment and theory can be attributed to correlations during the least-squares refinement, as well as the shape of the Laplacian function itself. It could be expected that the aromatic hydroxyl group, in which the hydrogen lies in the plane of the aromatic ring, would be of sp^2 type geometry having some interaction with the π-orbitals of the aromatic ring. However, the existence of two charge concentrations in the lone pair region is an indication that this interaction is not very significant.

Electrostatic Potential. The core structure of the estrogen molecule generally is hydrophobic and relatively predictable in terms of the electrostatic potential. The ESP plotted on the $\rho(\mathbf{r}) = 0$ .001 au molecular surface for the E_2 molecule with the program package gOpenMol[46] is shown in Figure 3 for both the experimental and theoretical results. This particular value of the electron density is the value most commonly used in the literature and the one Bader proposed in his original work on molecular surfaces.[47] Since the potential for the isolated molecule (taken from the crystal) has been calculated in this case, the ESP does not directly reflect the interactions in the condensed phase, such as hydrogen bonding. The negative

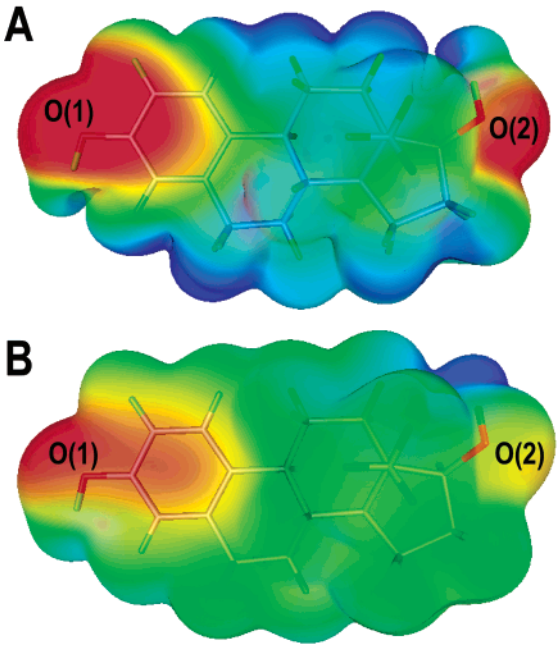

Figure 3. The electrostatic potential of a single E_2 molecule taken from the solid state plotted on the molecular ($\rho(\mathbf{r}) = 0.001$ au $= 0.00675$ e Å^{-3}) surface: (a) from the experimental data and (b) from the solid state theoretical data. Color scheme ranges from red (-0.15 e Å^{-1}) via green (zero) to blue (0.15 e Å^{-1}) (-48.3 to 48.3 kcal/(e·mol)).

potential areas (red) are produced by the aromatic ring and oxygen atoms (Figure 3), while the hydrogen atoms produce positive areas (blue) on the molecular surface with the molecular core being essentially neutral.

The hydroxyl groups are of particular interest in the E_2 molecule, offering varying environments being bound to sp^2 and sp^3 type carbons, and being involved in several hydrogen bonds. The consistency in the lone pair density, in shape, size, position (Figure 2, Table 6), and hydrogen-bonding geometry, suggested that the electrostatic potential surrounding the oxygen atoms might be relatively consistent in shape and magnitude. This, however, was not quite the case. Figure 4 demonstrates that the negative ESP area significantly extends around the O(1) atom linking with the negative area above and below the aromatic ring created by its π-density. A minimum ESP of ca. -0.49 e Å^{-1} was observed for this area.

Before discussing the O(2) hydroxyl group, it is important to recognize the orientation of the hydrogen atom H(2O). A hydroxyl group attached to an aromatic ring almost exclusively has the hydrogen atom in the plane of the ring. Obviously, a hydroxyl group bound to an sp^3 carbon can freely rotate. In the solid state, the orientation of the OH group will almost always be defined by the hydrogen-bonding scheme. Figure 5 displays the D-ring[48] of the E_2 molecule, and the torsion angle (γ) of 51° between H(2O) and H(17). The negative electrostatic potential around O(2) has a somewhat lower maximum value than that of the O(1) hydroxyl group, reaching a value of ca. -0.34 e Å^{-1}. The coverage area of the negative potential seems much smaller too.

These ESP distributions for both hydroxyl group regions are in very good agreement with the ESP previously calculated theoretically.[3,49] The negative ESP areas can be considered as possible locations of initial ligand−receptor electrostatic interactions at the early "recognition" stage.[50] Estrogen receptor−ligand final binding probably takes place through hydrogen bonding and van der Waals bond formation.[51] On the basis of competitive

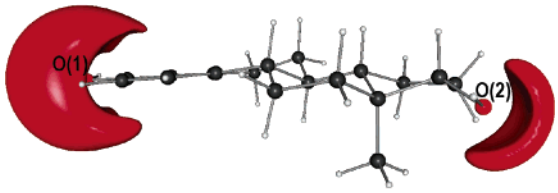

Figure 4. Electrostatic potential isosurface of a single E_2 molecule. The red surfaces represent -0.2 e Å^{-1}. The 3DPlot program[53] has been used.

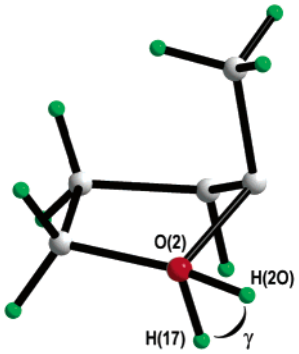

Figure 5. The D-ring projection down the O(2)−C(17) bond showing the torsion angle ($\gamma = 51°$) between the H(2O) and H(17) atoms.

TABLE 6: (3,+3) Critical Points in the Laplacian Associated with the Lone Pair Electron Concentrations of the Oxygen Atoms

atom	lone pair	$\nabla^2\rho(\mathbf{r}_c)$ (e Å^{-5})	O−LP (Å)	LP−O−LP (deg)	C−O−LP (deg)	H−O−LP (deg)
O(1)	LP1	−110	0.348	96	121	114
	LP2	−108	0.348	96	107	112
	LP1[a]	−140	0.338	106	108	110
	LP2[a]	−140	0.338	106	106	119
O(2)	LP3	−113	0.347	138	81	94
	LP4	−115	0.348	138	115	113
	LP3[a]	−150	0.336	128	106	106
	LP4[a]	−147	0.337	128	103	103
O(3)	LP5	−163	0.324	151	101	
	LP6	−177	0.328	151	104	
	LP5[a]	−141	0.336	143	106	
	LP6[a]	−133	0.337	143	111	

[a] The model obtained from the refinement over the theoretical data.

binding studies, the phenolic OH group of the E_2 molecule contributes ~1.9 kcal/mol to the binding free energy, the 17β-hydroxyl group ~0.6 kcal/mol, and the aromatic ring ~1.5 kcal/mol to the total of 12 kcal/mol.[52] The phenolic hydroxyl group is assumed to act mainly as a hydrogen bond donor, the 17β-hydroxyl group, probably, acts as a hydrogen bond acceptor, and the aromatic ring is suggested to have "weak polar interactions" with receptor residues.[52] Both the hydroxyl groups and the aromatic ring have significant negative ESP areas, which provide at least the initial driving force toward binding to these areas. High positive charges of H(1O) and H(2O) and highly negative charges of both oxygen atoms (Table 4) should provide strong hydrogen bonding to the estrogen receptor.

Conclusions

This is one of the few charge density studies accomplished for large (52 atoms) organic molecules in a noncentrosymmetric space group. Our study shows that it is possible to obtain quality diffraction data for such a system; an optimal coordinate system and slow, initially constrained refinement are necessary tools

for this type of study. Since most estrogens are identical in the core structure of the molecule, this study will provide a better starting point for future multipole refinements of other estrogen derivatives. Overall our results pertaining to the urea molecule reasonably agree with the previous literature results thus demonstrating confidence in our analysis.

For the E_2 molecule, the lone pair densities of the oxygen atoms, which are extremely small features of the system, were found to be quite similar. This indicates that the oxygen atom bound at the C(3) position does not have a strong interaction with the π-orbitals of the aromatic ring in the ground state configuration. Despite this consistency, the electrostatic potentials in the region of the hydroxyl groups differ in both shape and magnitude. Future studies may reveal how the H(17)−C(17)−O(2)−H(20) torsion angle affects the electrostatic potential of the C(17) hydroxyl group. Obviously, studies on many more estrogen systems must be completed before the comparative portion of the study can take place to determine the relationship between the electrostatic potential and estrogenic activity.

Acknowledgment. We would like to thank Dr. Samuel Brooks for his insight and encouragement in this study. We thank Dr. A. Stash and Prof. V. Tsirelson for making the programs WinXPRO and 3DPlot available for us and for valuable discussions. We appreciate the assistance of Dr. J. Overgaard in plotting the ESP on the molecular surface. We also thank the Department of Defense, USAMRMC, for financial support (Grants DAMD17-00-1-0468 and DAMD17-99-1-9408).

Supporting Information Available: Data collection strategy, theoretical and experimental CIF files, theoretical integrated atomic charges, local multipole coordinate system for the urea molecule, topological properties of bond critical points, and deformation and residual electron density maps. This material is available free of charge via the Internet at http://pubs.acs.org.

References and Notes

(1) Korach, K. S. *Science* **1994**, *266*, 1524−1527.
(2) Lacassagne, A. *Am. J. Cancer* **1936**, *27*, 217−225.
(3) VanderKuur, J. A.; Wiese, T.; Brooks, S. C. *Biochemistry* **1993**, *32*, 7002−7008. Brooks, S. C.; Skafar, D. F. *Steroids* **2004**, *69*, 401−418.
(4) Zhurova, E. A.; Matta, C. F.; Wu, N.; Zhurov, V. V.; Pinkerton, A. A. *J. Am. Chem. Soc.* **2006**, *128*, 8849−8861.
(5) Gutendorf, B.; Westendorf, J. *Toxicology* **2001**, *166*, 79−89.
(6) Nishihara, T.; Nishikawa, J.; Kanayama, T.; Dakeyama, F.; Saito, K.; Imagawa, M.; Takatori, S.; Kitagawa, Y.; Hori, S.; Utsumi, H. *J. Health Sci.* **2000**, *46*, 282−298.
(7) Zavodnik, V.; Stash, A.; Tsirelson, V.; De Vries, R.; Feil, D. *Acta Crystallogr.* **1999**, *B55*, 45−54.
(8) Gatti, C.; Saunders, V. R.; Roetti, C. *J. Chem. Phys.* **1994**, *101*, 10686−10696.
(9) Swaminathan, S.; Craven, B. M.; Spackman, M. A.; Stewart, R. F. *Acta Crystallogr.* **1984**, *B40*, 398−404.
(10) Dovesi, R.; Causa', M.; Orlando, R.; Roetti, C. *J. Chem. Phys.* **1990**, *92*, 7402−7411.
(11) Rodrigues, B. L.; Tellgren, R.; Fernandes, N. G. *Acta Crystallogr.* **2001**, *B57*, 353−358.
(12) Aray, Y.; Gatti, C.; Murgich, J. *J. Chem. Phys.* **1994**, *101*, 9800−9806.
(13) Spackman, M. A.; Byrom, P. G.; Alfredsson, M.; Hermansson, K. *Acta Crystallogr.* **1999**, *A55*, 30−47.
(14) de Vries, R. Y.; Feil, D.; Tsirelson, V. G. *Acta Crystallogr.* **2000**, *B56*, 118−123.
(15) Stevens, E. D.; Klein, C. L. *Transactions ACA* **1990**, *26*, 79−89.
(16) Duax, W. L. *Acta Crystallogr.* **1972**, *B28*, 1864−1871.
(17) *SAINT Software Package*; BRUKER-AXS: Madison, WI, 1999.
(18) Blessing, R. H. *J. Appl. Crystallogr.* **1997**, *30*, 421−42
(19) Sheldrick, G. M.; *SHELXTL*, V. 6.14, An Integrated System for Solving, Refining and Displaying Crystal Structures from Diffraction Data; University of Göttingen: Göttingen, Germany, 2000.
(20) Koritsanszky, T.; Richter, T.; Macci, P.; Gatti, C.; Howard, S.; Mallinson, P. R.; Farrugia, L.; Su, Z. W.; Hansen, N. K. *XD*, A Computer Program Package for Multipole Refinement and Analysis of Electron Densities from Diffraction Data, Tech. Rep.; Freie Universität Berlin: Berlin, Germany, 2003.
(21) Hansen, N.; Coppens, P. *Acta Crystallogr.* **1978**, *A34*, 909−921.
(22) Kirschbaum, K.; Kumaradhas, P.; Parrish, D.; Pinkerton, A. A.; Zhurova, E. A. *J. Appl. Crystallogr.* **2003**, *36*, 1464−1466.
(23) Allen, F. H.; Kennard, O.; Watson, D. G.; Brammer, L.; Orpen, A. G.; Taylor, R. *J. Chem. Soc., Perkin Trans. 2* **1987**, S1−S19.
(24) Saunders, V. R.; Dovesi, R.; Roetti, C.; Causà, M.; Harrison, N. M.; Orlando, R.; Sicovich-Wilson, C. M. *CRYSTAL98 User's Manual*; University of Torino: Torino, 1998.
(25) Coppens, P.; Guru Row, T. N.; Leung, P.; Stevens, E. D.; Becker, P. J.; Yang, Y. W. *Acta Crystallogr.* **1979**, *A35*, 63−72.
(26) Coppens, P. *X-Ray Charge Densities and Chemical Bonding*; Oxford University Press: New York, 1997.
(27) Volkov, A.; Abramov, Y. A.; Coppens, P. *Acta Crystallogr.* **2001**, *A57*, 272−282.
(28) Bader, R. F. W. *Atoms in Molecules*: *A Quantum Theory*; Oxford University Press: Oxford, UK, 1990.
(29) Stash, A. I.; Tsirelson, V. G. *J. Appl. Crystallogr.* **2002**, *35*, 371−373.
(30) Stash, A. I.; Tsirelson, V. G. *Crystallogr. Rep.* **2005**, *50*, 202−209.
(31) Critical points are special points in the electron density, where $\nabla\rho(\mathbf{r}_{CP}) = 0$. The saddle (3,−1) point reflects the chemical bonding.
(32) Bader, R. F. W. *Phys. Rev.* **1994**, *B49*, 13348−13356.
(33) A bond path is a line along which the electron density decreases for any lateral displacement.
(34) Bader, R. W. F. *J. Phys. Chem.* **1998**, *A102*, 7314−7323.
(35) Symmetry operations are the following: for H(1NB) $\{x, y, z\}$, for H(2NB) $\{-x, 0.5 + y, 0.5 - z - 1\}$, for H(1O) $\{0.5 - x - 2, -y - 1, 0.5 + z\}$, for H(2NA) $\{-x - 0.5, -y - 1, z + 0.5\}$, for H(2O) $\{0.5 - x, 0.5 + y - 1, -z - 1\}$, for H(1NA) $\{x, 0.5 - y - 2, -z\}$.
(36) Li, X.; Wu, G.; Abramov, Y. A.; Volkov, A. V.; Coppens, P. *Proc. Natl. Acad. Sci. U.S.A.* **2002**, *99*, 12132−12137.
(37) Flensburg, C.; Madsen, D. *Acta Crystallogr.* **2000**, *A56*, 24−28.
(38) Volkov, A.; Abramov, Yu.; Coppens, P.; Gatti C. *Acta Crystallogr.* **2000**, *A56*, 332−339.
(39) Tsirelson, V. G.; Stash, A. I.; Potemkin, V. A.; Rykounov, A. A.; Shutalev, A. D.; Zhurova, E. A.; Zhurov, V. V.; Pinkerton, A. A.; Gurskaya, G. V.; Zavodnik, V. E. *Acta Crystallogr.* **2006**, *B62*, 676−688.
(40) Destro, R.; Merati, F. *Z. Naturforsch.* **1993**, *48a*, 99−104.
(41) Ellena, J.; Goeta, A. E.; Howard, J. A. K.; Punte, G. *J. Phys. Chem. A* **2001**, *105*, 8696−8708.
(42) Hibbs, D. E.; Hanrahan, J. R.; Hursthouse, M. B.; Knight, D. W.; Overgaard, J.; Turner, P.; Piltz, R. O.; Waller, M. P. *Org. Biomol. Chem.* **2003**, *1*, 1034−1040.
(43) Dominiak, P. M.; Grech, E.; Barr, G.; Teat, S.; Mallinson, P.; Wozniak, K. *Chem. Eur. J.* **2003**, *9*, 963−970.
(44) Scheins, S.; Messerschmidt, M.; Luger, P. *Acta Crystallogr.* **2005**, *B61*, 443−448.
(45) Messerschmidt, M.; Scheins, S.; Luger, P. *Acta Crystallogr.* **2005**, *B61*, 115−121.
(46) http://www.csc.fi/gopenmol/.
(47) Bader, R. F. W.; Carroll, M. T.; Cheeseman, J. R.; Chang, C. *J. Am. Chem. Soc.* **1987**, *109*, 7968−7979.
(48) The C(13)-C(14)-C(15)-C(16)-C(17) ring.
(49) Kubli-Garfias, C. *J. Mol. Struct.* (*THEOCHEM*) **1998**, *452*, 175−183.
(50) Politzer, P.; Murray, J. S. *Theor. Chem. Acc.* **2002**, *108*, 134−142.
(51) Hu, J.-Y.; Aizawa, T. *Water Res.* **2003**, *37*, 1213−1222.
(52) Anstead, G. M.; Carlson, K. E.; Katzenellenbogen, J. A. *Steroids* **1997**, *62*, 268−303.
(53) Courtesy of Dr. A. Stash, 2006.